RSC Advances

PAPER

View Article Online
View Journal | View Issue

Check for updates

Cite this: *RSC Adv.*, 2017, **7**, 22243

Aromatic cage-like B_{46}: existence of the largest decagonal holes in stable atomic clusters†

Truong Ba Tai *[ab] and Minh Tho Nguyen [c]

Received 9th March 2017
Accepted 13th April 2017

DOI: 10.1039/c7ra02870a

rsc.li/rsc-advances

The most stable form of B_{46} has a cage-like structure containing two hexagonal, two heptagonal and two decagonal holes. The intriguing presence of decagonal holes is a remarkable breakthrough since such large holes have never been found before for atomic clusters. This finding not only provides more insights into the growth motif of large-sized boron clusters, but also presents a new family of cage-like boron clusters containing large B_N holes with $N = 6$–10.

Open Access Article. Published on 21 April 2017. Downloaded on 1/21/2026 12:05:50 AM.
This article is licensed under a Creative Commons Attribution 3.0 Unported Licence.

Introduction

Exhibiting a wide range and an unpredictability of structural characteristics, boron clusters are of great interest to theoretical and experimental scientists.[1–6] The early studies showed that small boron clusters at neutral state B_n ($n = 2$–19) have planar or quasi-planar structures containing basic triangular units.[1–3] At larger sizes, they exhibit more complex geometries, including convex structures or tubular shapes containing either two or three *N*-membered rings connected together in antiprism bonding motif and quasi-planar geometries containing *N*-membered holes ($N = 5$–8).[7,8] Interestingly, while their cationic state prefers the double-ring shapes at smaller sizes,[5,9] anionic species B_n^- remain the quasi-planar geometrical structures up to B_{40}^-.[10]

Stimulated by the discovery of carbon fullerene C_{60} (ref. 11) and its unique properties, the search for cage-like boron clusters has been greatly attractive over the last decade. The buckyball B_{80}, an isoelectronic species of the fullerene C_{60}, was proposed in 2007 (ref. 12) and has received much attention,[13,14] although recent theoretical studies reported that core–shell structures are more favourable in energy.[15] Recently, the B_{40} cluster was found as a stable all-boron fullerene containing four heptagonal holes and two hexagonal holes.[10,16,17] In the combined experimental and theoretical study, Wang *et al.*[10] reported that this caged structure was somewhat less stable than a quasi-planar structure containing two hexagonal holes and both of them were identified in the photoelectron spectrum. These findings marked a breakthrough in the discovery of boron clusters since the anion B_{40}^- is the first cage-like boron cluster which was observed in experiment. A few cage-like systems such as B_{38},[18] B_{39}^-, B_{41}^+ and B_{42}^{2+} were subsequently reported.[19] A common structural feature of these systems is that they are composed of the hexagonal and heptagonal holes. Smaller cage-like structures B_{14}, $B_{28}^{0/-}$ and B_{29}^- were also reported as smallest boron cages which were almost degenerate with the planar structures.[20,21] More recently, we found that the B_{42}^+ and B_{44} also have, for their lowest-energy form, cage-like structures which contain eight- and nine-membered holes, respectively (Fig. 1).[22] The neutral cage-like B_{42} is nearly degenerate with a triple ring tube of 14-atom strings. The presence of such large holes is intriguing since they have been found for the first time in atomic clusters, and has stimulated us to further explore larger sized species B_n to find out elements for the answer to the question as to whether boron clusters with larger holes exist.

In the present work, we report on the existence of the boron cluster B_{46} which exhibits a cage-like structure containing two hexagonal, two heptagonal and two decagonal (ten-membered) holes. The presence of decagonal holes has never been found before in atomic clusters, of either main group elements or transition metals. The present work does not only provide more

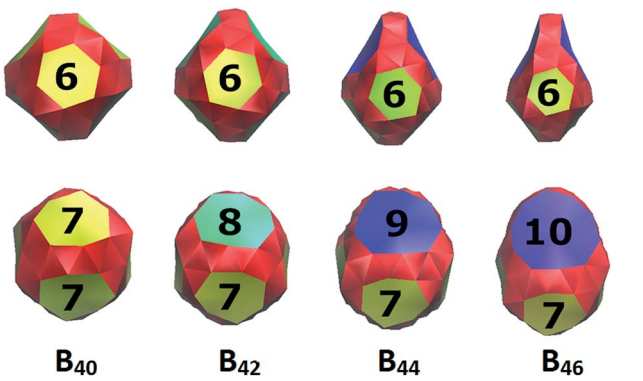

Fig. 1 Shape of the most stable structures of B_n with $n = 40$, 42, 44 and 46.

[a]Computational Chemistry Research Group, Ton Duc Thang University, Ho Chi Minh City, Vietnam. E-mail: truongbatai@tdt.edu.vn

[b]Faculty of Applied Sciences, Ton Duc Thang University, Ho Chi Minh City, Vietnam

[c]Department of Chemistry, KU Leuven, Leuven City, Belgium

† Electronic supplementary information (ESI) available. See DOI: 10.1039/c7ra02870a

Open Access Article. Published on 21 April 2017. Downloaded on 1/21/2026 12:05:50 AM.
This article is licensed under a Creative Commons Attribution 3.0 Unported Licence.

insight into the growth motif of boron clusters, but it also shows a new family of cage-like boron clusters containing large hole B_N with $N = 6$–10 (Fig. 1).

Computational methods

Extensive structural searches for B_{46} were carried out by using stochastic random searching procedures,[23] and manual structural construction based on the known structures of smaller sized boron clusters[17–19,22] by using the PBE0 functional[24] in conjunction with small basis set 3-21G.[25] Low-lying isomers B_{46} with relative energy of 0.0–5.0 eV obtained from initial geometry optimizations at the PBE0/3-21G were fully re-optimized at the higher level PBE0/6-311+G(d).[26] To identify a true global minimum, single-point electronic energies of a few lowest-lying B_{46} isomers were subsequently calculated using the couple-cluster theory CCSD(T)/6-31G(d) method[27] at their PBE0/6-311+G(d) optimized geometries. These computational methods were used to effectively establish the energy landscape of boron clusters in the literature.[3,4,7–9,22] All calculations were performed using the Gaussian 09 (ref. 28) and Molpro 2009 packages.[29]

Results and discussion

Identification of the global minimum for B_{46} was carried out using the DFT and CCSD(T) methods. The optimized geometries and relative energies (eV) of a few lowest-lying B_{46} isomers are depicted in Fig. 2, while those of less stable isomers are shown in Fig. S1 of the (ESI†) file. At the CCSD(T)/6-31G(d)//PBE0/6-311+G(d) level, our computed results show that structure **I** (C_2, ^{1}A) which contains two hexagonal, two heptagonal and two decagonal holes is the most stable form. This structure is composed of 54 triangular units and six polygonal holes. The latter includes two decagonal B_{10}, two heptagonal B_7 and two hexagonal B_6 holes. This isomer can be constructed by replacing two neighboured heptagonal B_7 holes of the B_{40} fullerene by two decagonal B_{10} holes and following the Euler's rule for a polyhedron: E(104 edges) = F(54 triangular + 2 hexagonal + 2 heptagonal + 2 decagonal faces) + V(46 vertices) − 2.

Although a quasi-planar structure **II** (C_{2v}, $^1A_1$) which contains one hexagonal hole is more stable at the PBE0/6-311+G(d) level, it is 0.53 eV less stable than **I** at the CCSD(T)/6-31G(d). These calculated results are consistent with the early reports that the PBE0 tends to overestimate the cohesive energy of the quasi-planar or planar structures.[9,30] The next isomers exhibit different structural characteristics, including a quasi-planar structure **III** (C_1, ^{1}A), a tubular form **IV** (C_s, ^{1}A′) and cage-like structures **V** (C_1, ^{1}A) and **VI** (C_1, ^{1}A), with relative energies of at least 0.72 eV at the CCSD(T)/6-31G(d) level. The structure **III** is also quasi-planar structure containing two hexagonal hole, while the structure **IV** is tubular form which is composed of two fifteen-membered rings and one sixteen-membered ring.

As shown in Fig. 1, the clusters B_{40}, B_{42}, B_{44} and B_{46} have similar geometries in which two neighboured B_7 holes of B_{40} were replaced by two B_8, B_9 and B_{10} holes to form the B_{42}, B_{44} and B_{46}, respectively. We expect that these large-sized holes play as stable units in the building up of larger boron clusters.

To gain more understanding about the high stability of the isomer **I**, we performed molecular dynamics (MD) simulation for this system by using the CP2K programs.[31] The simulation was carried out at temperature of 500 K during a time of 30 ps using the PBE functional in conjunction with the 6-31G(d) basis set. RMSD values were calculated using the VMD code[32] and their plots are depicted in Fig. 3 together with the movie of simulation trajectory at 500 K (ESI†). During the BO-MD simulation at 500 K, the isomer **I** retains its connectivity pattern and cage-like shape with two decagonal holes. The root mean square deviation (RMSD) varies in range of 0.11 to 0.26 Å. The high stability of decagonal holes is of fundamental characteristic and gives us more understanding about the growth mechanism of boron clusters.

The characteristics of electron delocalization and aromaticity of boron clusters have attracted much attention since they provide us with better understanding about their stability. The

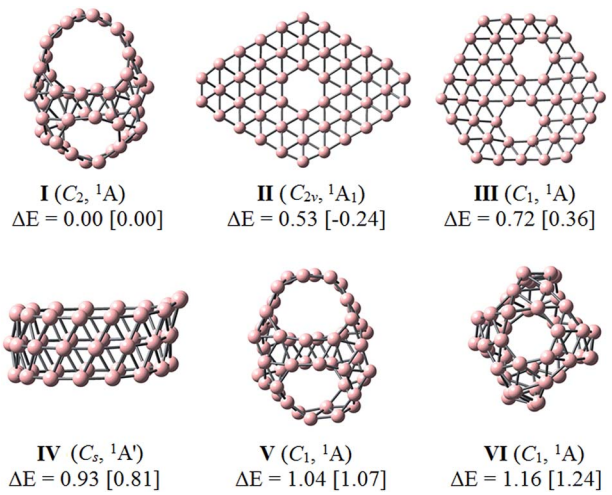

Fig. 2 Optimized geometries and relative energies (eV) of the lowest-lying isomers B_{46} obtained at the CCSD(T)/6-31G(d)//PBE0/6-311+G(d) level of theory (in square brackets are PBE0/6-311+G(d) values).

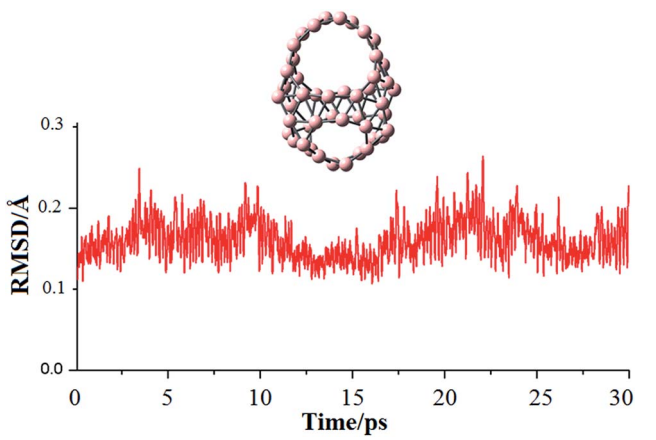

Fig. 3 Born–Oppenheimer molecular simulation of the lowest isomer B_{46} at 500 K.

This journal is © The Royal Society of Chemistry 2017

Open Access Article. Published on 21 April 2017. Downloaded on 1/21/2026 12:05:50 AM.
This article is licensed under a Creative Commons Attribution 3.0 Unported Licence.

aromatic feature of B_{46} is first evaluated using the nucleus independent chemical shift (NICS)[33] which is one common criterion to evaluate the molecular aromaticity. Our NICS calculations at the central position of structure **I** point out that this cage is highly aromatic with a large negative NICS value of −26 ppm. This value is comparable to the NICS values obtained earlier for boron cages, *e.g.* −38 ppm for B_{39}^-,[19a] −42 ppm for B_{40} (ref. 10) and −21 ppm for B_{44}.[22a] In the previous report, using the profiles of the z-component of the induced magnetic field (B_z^{ind}), Merino *et al.*[17a] showed that the intensity of B_z^{ind} in B_{40} diminishes gradually along the center to the surface of cage B_{40}. Based on the computed B_z^{ind} profiles, these authors also indicated that there is strong delocalization in σ-electron systems of both 6- and 7-membered rings. While the π-electron system of the 6-membered rings presents strong delocalization, the π-electron delocalization of the 7-membered rings is much less.

To have more insight into the high stability and aromaticity of **I**, we performed a topological analysis of the electron localization function (ELF).[34] This approach does not only give us a general view of bonding pattern and electron distribution, but also allows the aromatic feature of the systems to be examined on the basis of their bifurcation values of the ELF_σ and ELF_π components.[7,22,35] Accordingly, each total ELF map can be partitioned in terms of separate ELF_σ and ELF_π components that arise from the contributions of σ and π electrons, respectively. An aromatic system possesses a high ELF bifurcation value, whereas the corresponding bifurcation value is low in an anti-aromatic system. The ELF analysis was carried out by using the Dgrid-4.6 package.[36]

Our analysis of canonical molecular orbitals (CMOs) for **I** shows that this species contains a total of 69 valence MOs which are separated into 55 σ-MOs and 14 π-MOs. The ELF_π and ELF_σ plots depicted in Fig. 4 emphasize an excellent electron delocalization for both σ and π electron systems of cage-like structure **I**. At the value of $ELF_\sigma = 0.85$, the isosurface of the ELF_σ is separated into 54 basins that determine the chemical bonding of 54 triangular units. The isosurface of ELF_π is separated at the bifurcation value of $ELF_\pi = 0.70$ which consequently indicates a π electron delocalization over the whole system. In general, such an electron distribution with high bifurcation values gives raise to two highly delocalized σ and π bonding systems, which make the isomer **I** aromatic and thereby highly thermodynamically stable.

To probe a better understanding about the chemical bonding characteristic of the B_{46}, the further analysis was carried out for the most stable isomer **I** by using adaptive natural density partitioning (AdNDP) method.[37] This approach was effectively used to analyze the chemical bonds of boron clusters in the early reports.[4c,10,19] As shown in Fig. 5, 69 valence electron pairs of the isomer **I** are almost delocalized over structure and form 55 σ-bonds and 14 π-bonds. First set includes 46(3c–2e) σ-bonds (Fig. 5a) and 8(6c–2e) σ-bonds (Fig. 5b) which distribute on 54 triangle units. The remaining (6c–2e) σ-bond is located at top of structure (Fig. 5b) that supports for high stability of two ten-membered rings.

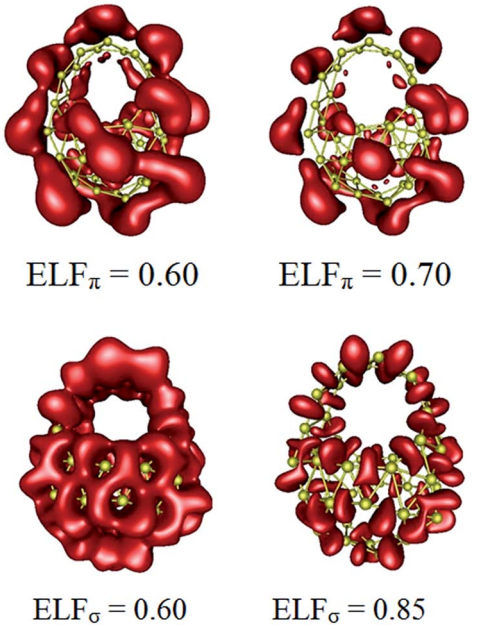

Fig. 4 Plots of ELF_π (up) and ELF_σ (down) of the cage-like structure **I**.

Interestingly, second set includes 4 (5c–2c) π-bonds and 10 (6c–2e) π-bonds that are delocalized over planar boron double chains (BDCs) of the B_{46} (Fig. 5c). This delocalized σ and π-bonding pattern agrees well with our above ELF analysis and strongly supports for high stability of the B_{46} **I**.

The vibrational spectrum is interesting and helpful since it allows us to identify structural characteristics. To assist future experimental studies, simulations of infrared (IR) spectra of two stable lowest-lying isomers **I** and **II** obtained at the PBE0/6-311+G(d) level are shown in Fig. 6. While the IR spectrum of the planar structure **II** exhibits many intensive peaks in a large range of 500–1400 cm^{-1}, the spectrum of **I** is more concentrated in the range of 1200–1400 cm^{-1} and characterized by much less intensive peaks at low frequencies. For isomer **I**, seven major peaks appear at 381, 621, 799, 1029, 1232, 1293 and 1355 cm^{-1} which correspond to the intense peaks centered of 380, 713 and 1274 cm^{-1} of the cage B_{40},[17] and the peaks of 390, 776, 1005, 1231, 1275 cm^{-1} of the cage-like B_{44}.[22]

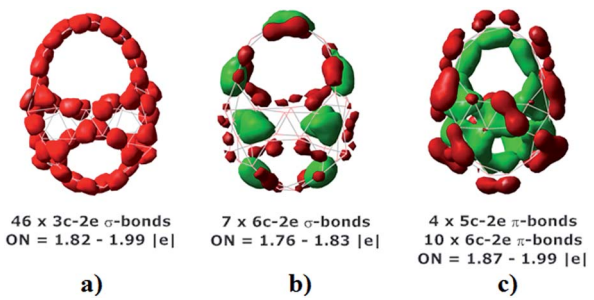

Fig. 5 The AdNDP bonding pattern of isomer **I** with occupation number (ON).

Open Access Article. Published on 21 April 2017. Downloaded on 1/21/2026 12:05:50 AM.
This article is licensed under a Creative Commons Attribution 3.0 Unported Licence.

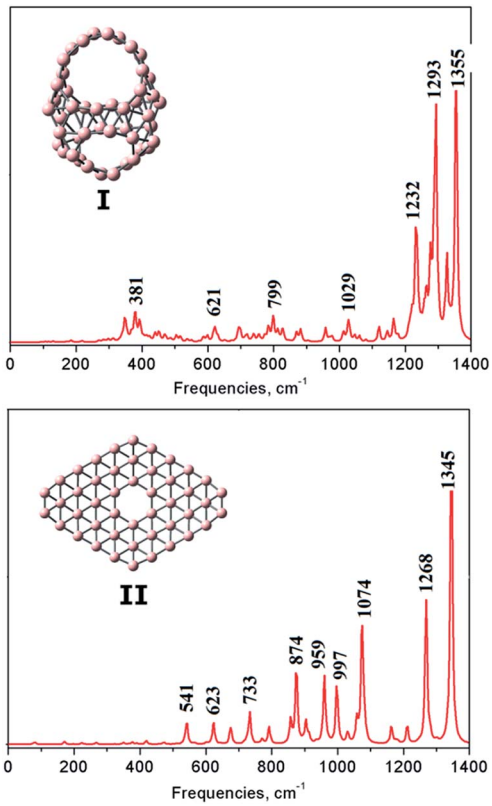

Fig. 6 Simulated infrared spectra of the lowest-lying B_{46} isomers.

Conclusions

In conclusion, we performed a theoretical study on the B_{46} cluster by using DFT and CCSD(T) methods, and found that the most stable form of B_{46} is the cage-like structure **I** containing two decagonal, two heptagonal and two hexagonal holes. The structure **I** is composed of two delocalized σ and π bonding systems that rationalize its high stability. BO-MD simulations at 500 K showed that the B_{46} is both thermodynamically and kinetically stable. The analysis of chemical bonding characteristics showed that the B_{46} contains two delocalization σ and π electron systems that supports for its enhanced stability. The presence of decagonal holes again marks a breakthrough since it has been never found before in elemental clusters. The present work does not only provide more insight into the growth motif of boron clusters, but it also emphasizes a new family of cage-like boron clusters containing large holes B_N with $N = 6$–10.

Acknowledgements

We are indebted to the KU Leuven Research Council (GOA program) and Vlaams Supercomputer Centrum (VSC).

Notes and references

1 (*a*) I. Boustani, Z. Zhu and D. Tomanek, *Phys. Rev. B: Condens. Matter Mater. Phys.*, 2011, **83**, 193405; (*b*) I. Boustani, *Chem. Modell.*, 2011, **8**, 1; (*c*) S. Chacko, D. G. Kanhere and I. Boustani, *Phys. Rev. B: Condens. Matter Mater. Phys.*, 2003, **68**, 035414.

2 (*a*) W. L. Li, Y. F. Zhao, H. S. Hu, J. Li and L. S. Wang, *Angew. Chem., Int. Ed.*, 2014, **53**, 5540; (*b*) C. Romanescu, D. J. Harding, A. Fielicke and L. S. Wang, *J. Chem. Phys.*, 2012, **137**, 014317; (*c*) A. N. Alexandrova, A. I. Boldyrev, H.-J. Zhai and L.-S. Wang, *Coord. Chem. Rev.*, 2006, **250**, 2811; (*d*) Z. A. Piazza, I. A. Popov, W.-L. Li, R. Pal, X. C. Cheng, A. I. Boldyrev and L. S. Wang, *J. Chem. Phys.*, 2014, **141**, 034303; (*e*) I. A. Popov, Z. A. Piazza, W. L. Li, L. S. Wang and A. I. Boldyrev, *J. Chem. Phys.*, 2013, **139**, 144307; (*f*) W. Huang, A. P. Sergeeva, H. J. Zhai, B. B. Averkiev, L. S. Wang and A. I. Boldyrev, *Nat. Chem.*, 2010, **2**, 202.

3 (*a*) A. G. Arvanitidis, T. B. Tai, M. T. Nguyen and A. Ceulemans, *Phys. Chem. Chem. Phys.*, 2014, **16**, 18311; (*b*) T. B. Tai, A. Ceulemans and M. T. Nguyen, *Chem.–Eur. J.*, 2012, **18**, 4510; (*c*) H. T. Pham, L. V. Duong, B. Q. Pham and M. T. Nguyen, *Chem. Phys. Lett.*, 2013, **557**, 32; (*d*) T. B. Tai, D. J. Grant, M. T. Nguyen and D. A. Dixon, *J. Phys. Chem. A*, 2010, **114**, 994; (*e*) T. B. Tai, N. M. Tam and M. T. Nguyen, *Chem. Phys. Lett.*, 2012, **530**, 71.

4 (*a*) J. O. C. Jimenez-Halla, R. Islas, T. Heine and G. Merino, *Angew. Chem., Int. Ed.*, 2010, **49**, 5668; (*b*) D. Moreno, S. Pan, L. Liu-Zeonjuk, R. Islas, E. Osorio, G. M. Guajardo, P. K. Chattaraj, T. Heine and G. Merino, *Chem. Commun.*, 2014, **50**, 8140; (*c*) F. Cervantes-Navarro, G. Martinez-Guajardo, E. Osorio, D. Moreno, W. Tiznado, R. Islas, K. J. Donald and G. Merino, *Chem. Commun.*, 2014, **50**, 10680; (*d*) G. Martinez-Guajardo, A. P. Sergeeva, A. I. Boldyrev, T. Heine, J. M. Ugalde and G. Merino, *Chem. Commun.*, 2011, **47**, 6242; (*e*) S. Jalife, L. Liu, S. Pan, J. L. Cabellos, E. Osorio, C. Lu, T. Heine, K. J. Donald and G. Merino, *Nanoscale*, 2016, **8**, 17639.

5 E. Oger, N. R. M. Crawford, R. Kelting, P. Weis, M. M. Kappes and R. Ahlrichs, *Angew. Chem., Int. Ed.*, 2007, **46**, 8503.

6 (*a*) S. Li, Z. Zhang, Z. Long, G. Sun and S. Qin, *Sci. Rep.*, 2016, **6**, 1; (*b*) A. B. Rahane and V. Kumar, *Nanoscale*, 2015, **7**, 4055.

7 (*a*) T. B. Tai, L. V. Duong, H. T. Pham, D. T. T. Mai and M. T. Nguyen, *Chem. Commun.*, 2014, **50**, 1558; (*b*) T. B. Tai and M. T. Nguyen, *Chem. Commun.*, 2015, **51**, 7677; (*c*) T. B. Tai and M. T. Nguyen, *Phys. Chem. Chem. Phys.*, 2015, **17**, 13672.

8 (*a*) Z. A. Piazza, H.-S. Hu, W.-L. Li, Y.-F. Zhao, J. Li and L.-S. Wang, *Nat. Commun.*, 2014, **5**, 31; (*b*) W. L. Li, Q. Chen, W. J. Tian, H. Bai, Y. F. Zhao, H. S. Hu, J. Li, H. J. Zhai, S. D. Li and L. S. Wang, *J. Am. Chem. Soc.*, 2014, **126**, 12257; (*c*) B. Kiran, S. Bulusu, H.-J. Zhai, S. Yoo, X. C. Zeng and L. S. Wang, *Proc. Natl. Acad. Sci. U. S. A.*, 2005, **102**, 961.

9 T. B. Tai, N. M. Tam and M. T. Nguyen, *Theor. Chem. Acc.*, 2012, **131**, 1241.

10 H.-J. Zhai, Y.-F. Zhao, W.-L. Li, Q. Chen, H. Bai, H.-S. Hu, Z. A. Piazza, W.-J. Tian, H.-G. Lu, Y.-B. Wu, Y.-W. Mu, G.-F. Wei, Z.-P. Liu, J. Li, S.-D. Li and L.-S. Wang, *Nat. Chem.*, 2014, **6**, 727.

11 H. W. Kroto, J. R. Heath, S. C. O'Brien, R. F. Curl and R. E. Smalley, *Nature*, 1985, **318**, 162.

 This journal is © The Royal Society of Chemistry 2017

Open Access Article. Published on 21 April 2017. Downloaded on 1/21/2026 12:05:50 AM.
This article is licensed under a Creative Commons Attribution 3.0 Unported Licence.

12 N. G. Szwacki, A. Sadrzadeh and B. I. Yakobson, *Phys. Rev. Lett.*, 2007, **98**, 166804.
13 (*a*) A. Ceulemans, J. T. Muya, G. Gopakumar and M. T. Nguyen, *Chem. Phys. Lett.*, 2008, **461**, 226; (*b*) J. T. Muya, E. Lijnen, M. T. Nguyen and A. Ceulemans, *Chem. Phys. Chem.*, 2013, **14**, 346.
14 (*a*) S. De, A. Willand, M. Amsler, P. Pochet, L. Genoverse and S. Grodecker, *Phys. Rev. Lett.*, 2011, **106**, 225502; (*b*) Y. Li, G. Zhou, J. Li, B.-L. Gu and W. Duan, *J. Phys. Chem. C*, 2008, **112**, 19268.
15 H. Li, N. Shao, B. Shang, L. F. Yuan, J. L. Yang and X. C. Zeng, *Chem. Commun.*, 2010, **46**, 387.
16 H. T. Pham, L. V. Duong, N. M. Tam, M. P. Pham-Ho and M. T. Nguyen, *Chem. Phys. Lett.*, 2014, **608**, 295.
17 (*a*) G. Martinez-Guajardo, J. L. Cabellos, A. Diaz-Celaya, S. Pan, R. Islas, P. K. Chattaraj, T. Heine and G. Merino, *Sci. Rep.*, 2015, **5**, 11287; (*b*) R. He and X. C. Zeng, *Chem. Commun.*, 2015, **51**, 3185.
18 (*a*) J. Lv, Y. Wang, L. Zhu and Y. Ma, *Nanoscale*, 2014, **6**, 11692; (*b*) T. B. Tai and M. T. Nguyen, *Nanoscale*, 2015, **7**, 3316.
19 (*a*) Q. Chen, W. L. Li, Y. F. Zhao, S. Y. Zhang, H. S. Hu, H. Bai, H. R. Li, W. J. Tian, H. G. Lu, H. J. Zhai, S. D. Li and L. S. Wang, *ACS Nano*, 2015, **9**, 754; (*b*) Q. Chen, S. Y. Zhang, H. Bai, W. J. Tian, T. Gao, H. R. Li, C. Q. Miao, Y. W. Mu, H. G. Lu, H. J. Zhai and S. D. Li, *Angew. Chem., Int. Ed.*, 2015, **54**, 8160.
20 (*a*) L. Cheng, *J. Chem. Phys.*, 2012, **136**, 104301; (*b*) J. Zhao, X. Huang, R. Shi, H. Liu, Y. Su and R. B. King, *Nanoscale*, 2015, **7**, 15086.
21 (*a*) Y. J. Wang, Y. F. Zhao, W. L. Li, T. Jian, Q. Chen, X. R. You, T. Ou, X. Y. Zhao, H. J. Zhai, S. D. Li and L. S. Wang, *J. Chem. Phys.*, 2016, **144**, 064307; (*b*) H. R. Li, T. Jian, W. L. Li, C. Q. Miao, Y. J. Wang, Q. Chen, X. M. Luo, K. Wang, H. J. Zhai, S. D. Li and L. S. Wang, *Phys. Chem. Chem. Phys.*, 2016, **18**, 29147.
22 (*a*) T. B. Tai and M. T. Nguyen, *Chem. Commun.*, 2016, **52**, 1652; (*b*) T. B. Tai and M. T. Nguyen, *Phys. Chem. Chem. Phys.*, 2016, **18**, 11620.
23 T. B. Tai and M. T. Nguyen, *J. Chem. Theory Comput.*, 2011, **7**, 1119.
24 (*a*) J. P. Perdew, K. Burke and M. Ernzerhof, *Phys. Rev. Lett.*, 1996, **77**, 3865; (*b*) J. P. Perdew, K. Burke and M. Ernzerhof, *Phys. Rev. Lett.*, 1997, **78**, 1396; (*c*) J. A. Pople, *J. Chem. Phys.*, 1980, **72**, 650.
25 (*a*) J. S. Binkley, J. A. Pople and W. J. Hehre, *J. Am. Chem. Soc.*, 1980, **102**, 939; (*b*) M. S. Gordon, J. S. Binkley, J. A. Pople, W. J. Pietro and W. J. Hehre, *J. Am. Chem. Soc.*, 1982, **104**, 2797; (*c*) K. D. Dobbs and W. J. Hehre, *J. Comput. Chem.*, 1987, **8**, 861.
26 (*a*) A. D. McLean and G. S. Chandler, *J. Chem. Phys.*, 1980, **72**, 5639; (*b*) K. Raghavachari, J. S. Binkley, R. Seeger and J. A. Pople, *J. Chem. Phys.*, 1980, **72**, 650.
27 M. Rittby and R. J. Bartlett, *J. Phys. Chem.*, 1988, **92**, 3033.
28 M. J. Frisch, *et al.*, *Gaussian 09, Revision C.01*, Gaussian, Inc., Wallingford CT, 2009.
29 H. J. Werner, *et al.*, *MOLPRO 09, version 2009.1*, 2009, see, http://www.molpro.net.
30 F. Li, P. Jin, D. Jiang, L. Wang, S. B. Zhang, J. Zhao and Z. Chen, *J. Chem. Phys.*, 2012, **136**, 074302.
31 J. Vande Vonele, M. Krack, F. Mohamed, M. Parrinello, Y. Chassaing and J. Hutter, *Comput. Phys. Commun.*, 2005, **8**, 1314.
32 W. Humphrey, A. Dalke and K. Schulten, *J. Mol. Graphics*, 1996, **14**, 33.
33 P. V. R. Schleyer, C. Maerker, A. Dransfeld, H. Jiao and N. J. V. E. Hommes, *J. Am. Chem. Soc.*, 1996, **118**, 6317.
34 A. Becke and K. Edgecombe, *J. Chem. Phys.*, 1990, **92**, 5397.
35 J. C. Santos, W. Tznado, R. Contreras and P. Fuentealba, *J. Chem. Phys.*, 2004, **120**, 1670.
36 M. Kohout, Dgrid-4.6, Radebeul, 2011.
37 D. Y. Zubarev and A. I. Boldyrev, *Phys. Chem. Chem. Phys.*, 2008, **10**, 5207.